Reduced Inhibition in an Animal Model of Cortical Dysplasia

Wei Jian Zhu[1] **and Steven N. Roper**[1,2]

[1]*Department of Neurological Surgery, University of Florida, and* [2]*Malcolm Randall Veterans Administration Medical Center, Gainesville, Florida 32610-0265*

Cortical dysplasia has a strong association with epilepsy in humans, but the underlying mechanisms for this are poorly understood. *In utero* irradiation of rats produces diffuse cortical dysplasia and neuronal heterotopia in the neocortex and hippocampus. Using *in vitro* neocortical slices, whole-cell patch-clamp recordings were obtained from pyramidal neurons in dysplastic cortex and control neocortex. Spontaneous IPSCs were reduced in amplitude (35%) and frequency (70%) in pyramidal cells from dysplastic cortex. Miniature IPSCs were reduced in frequency (66%) in dysplastic cortex. Two additional measures of cortical inhibition, monosynaptic evoked IPSCs and paired pulse depression of evoked EPSCs, were also impaired in dysplastic cortex. Spontaneous EPSCs were increased in amplitude (42%) and frequency (77%) in dysplastic cortex, but miniature EPSCs were not different between the two groups. These data demonstrate significant physiological impairment in inhibitory synaptic transmission in experimental cortical dysplasia. This supports previous immunohistochemical findings in this model and observations in humans of a reduction in the density of inhibitory interneurons in dysplastic cortex.

Key words: cortical dysplasia; GABA; neocortex; development; local circuits; epilepsy

Disorders of cortical development are common findings in people with intractable epilepsy and impaired cognitive development (Taylor et al., 1971; Palmini et al., 1991; Raymond et al., 1995). Cortical dysplasia is one type of such disorders and is characterized by loss of normal lamination in the neocortex, abnormal spatial orientation of the neurons, cytoskeletal abnormalities, and abnormalities of cell commitment (Mischel et al., 1995). Despite a strong association between cortical dysplasia and epilepsy, the exact relationship between structural abnormalities and seizure activity is not clear. A causal relationship between some types of focal cortical dysplasia and epilepsy is suggested by the fact that surgical resection of these lesions can abolish the person's seizures (Hirabayashi et al., 1993; Palmini et al., 1995). In other cases, cortical dysplasia can be present in people who never have seizures.

A number of animal models have been used to examine genetic control of cortical development and response to early cortical injury and to relate structural features of cortical dysplasia with functional abnormalities. *In utero* irradiation of rats is one such model. Exposure of pregnant rats and their fetuses to external irradiation on gestational day 17 produces offspring with microcephaly, diffuse cortical dysplasia, subcortical and periventricular heterotopic gray matter, heterotopic neurons in the hippocampus, and agenesis or hypoplasia of the corpus callosum (Riggs et al., 1956; Cowan and Geller, 1960; Roper et al., 1995). Previous studies have shown that the affected rats have an increased propensity for electrographic seizures in the presence of certain sedating agents (Roper et al., 1995). *In vitro* slices of dysplastic neocortex demonstrate enhanced epileptiform activity in the presence of the $GABA_A$ receptor antagonist bicuculline methiode when compared with control neocortex (Roper et al., 1997b). Immunohistochemical studies have demonstrated a selective reduction in inhibitory interneurons (cells immunoreactive for parvalbumin and calbindin-D28k) in dysplastic cortex (Roper et al., 1999). The current study was performed to study possible alterations in excitatory and inhibitory connections in cortical dysplasia using whole-cell patch-clamp recordings of spontaneous and evoked postsynaptic currents. We present evidence for a significant reduction in inhibitory connections in experimental cortical dysplasia when compared with control neocortex.

Received July 11, 2000; revised Sept. 7, 2000; accepted Sept. 20, 2000.

This work was supported by National Institute of Neurological Disorders and Stroke Grant NS35651 to S.N.R. Special thanks to Dr. F. E. Dudek for critiques and suggestions and Dr. Frank Bova for assistance with irradiation.

Correspondence should be addressed to Dr. Steven N. Roper, Department of Neurological Surgery, University of Florida, P.O. Box 100265, Gainesville, FL 32610-0265. E-mail: roper@neurosurgery.ufl.edu.

MATERIALS AND METHODS

Animals and irradiation. All procedures used in the study adhered to guidelines approved by the Institutional Animal Care and Use Committee at the University of Florida. Female Sprague Dawley rats with known insemination times were obtained (Harlan Sprague Dawley, Indianapolis, IN). The day of insemination was designated embryonic day 0 (E0). Pregnant rats were housed separately, and pups were weaned at postnatal day 28. All animals were maintained on 12 hr light/dark cycles and were provided food and water *ad libitum*. Offspring from six irradiated ($n = 20$ animals) and seven control ($n = 21$ animals) mothers were used for the experiments. Irradiation was performed on E17. Pregnant rats were placed in a Plexiglas box to limit movement and exposed to 225 cGy of external γ irradiation from a linear accelerator source.

Brain slice preparation. In vitro brain slices were obtained from 28- to 35-d-old rats using procedures similar to those described previously (Roper et al., 1997b). After decapitation, the brain was rapidly removed and submerged in ice-cold artificial CSF (ACSF) containing (in mM): NaCl 124, KCl 2.5, KH_2PO_4 1.25, $MgCl_2$ 2.5, $CaCl_2$ 0.5, $NaHCO_3$ 26, and glucose 10, pH 7.4 (300 mOsm/kg). Three hundred- to 400-μm-thick, coronal, hemispheric brain slices were obtained at the rostrocaudal level of the anterior commissure using a Vibratome (Campden Instruments). The slices were incubated in oxygenated (5% CO_2 and 95% O_2) ACSF at 32–34°C for 30 min and then maintained at room temperature (22–25°C) until they were transferred to a submersion-type recording chamber.

Electrophysiological recording. Neocortical pyramidal neurons were identified using infrared differential interference contrast (IR-DIC) videomicroscopy with a fixed-stage microscope (Axioskop-FS, equipped with a 40×, 0.80 W water-immersion lens; Zeiss, Oberkochen, Germany), according to their characteristic somata and apical dendrites. All of the recordings were made at room temperature (22–25°C) from slices kept under constant (2–3 ml/min) perfusion of ACSF as given above, with the exception that $MgCl_2$ and $CaCl_2$ concentrations were 1 and 2 mM, respectively. Drugs were applied to slices by gravity perfusion. Evoked synaptic responses were obtained in neocortical pyramidal cells using a twisted platinum-iridium wire (diameter, 76 μm) with current pulses (0–500 μA; duration, 0.1 msec) applied to the white matter adjacent to the recorded cell. Analysis of all evoked responses was based on averages of 10 trials per event with 30 sec intervals between stimuli.

Spontaneous and miniature postsynaptic currents. Tight-seal (>1 GΩ) whole-cell recordings were obtained from the cell body of neocortical pyramidal cells. Patch electrodes had a resistance of 3–5 MΩ when filled with (in mM): potassium gluconate 120, NaCl 8, HEPES 10, MgATP 4, Na_3GTP 0.4, EGTA 0.2, and biocytin 0.1%, pH 7.2 (280 mOsm/kg) for EPSCs and CsCl 125, HEPES 10, MgATP 5, Na_3GTP 0.4, $MgCl_2$ 4, EGTA 5, and biocytin 0.1%, pH 7.2 (280 mOsm/kg) for IPSCs. Neurons were voltage-clamped at −65 mV (for EPSCs) or −60 mV (for IPSCs) using an Axopatch 1D amplifier (Axon Instruments, Foster City, CA). Access resistance (10–25 MΩ) was monitored regularly during recordings, and cells were rejected if it changed >15% during the experiment. Data

were filtered at 2 kHz, digitized at 10 kHz, and stored in a computer using pClamp 8 software (Axon Instruments) for off-line data analysis. In some experiments, inhibitory currents were blocked using the $GABA_A$ receptor antagonists picrotoxin (100 μM) and bicuculline methiodide (BMI; 10 μM). $GABA_A$-gated IPSCs were recorded in the presence of DL-2-amino-5-phosphonopentanoic acid (AP-5; 50 μM) and 6-cyano-7-nitroquinoxaline-2,3-dione (CNQX; 10 μM) in the bath solution to block fast glutamatergic transmission. Miniature EPSCs (mEPSCs) and mIPSCs were recorded in the presence of tetrodotoxin (TTX; 1 μM).

Histology. Slices with biocytin-filled cells were fixed by immersion in 4% paraformaldehyde in 0.15 M phosphate buffer overnight at 4°C and then rinsed three times in PBS (0.01 M). The slices were incubated in PBS containing 10% methanol and 3% H_2O_2 for 1 hr to remove endogenous peroxidase activity and rinsed three times in PBS. Slices with biocytin-filled cells were then incubated in avidin–biotin–horseradish peroxidase complex (ABC Elite kit; Vector Laboratories, Burlingame, CA) in PBS (1:100), pH 7.3, containing 2% Triton X-100 for 48–72 hr at 4°C. The slices were rinsed and reacted with 3,3′-diaminobenzidine tetrahydrochloride (0.06%) and H_2O_2 (0.003%) in PBS, pH 7.4. The slices were mounted on subbed slides, air-dried overnight, dehydrated through a graded series of ethanols (70–100%), and coverslipped.

Data analysis and statistics. Event analysis was performed on continuous segments of spontaneous synaptic current records (sIPSCs, mIPSCs, sEPSCs, and mEPSCs) lasting 3–5 min in a semiautomated manner. Histograms were made of two parameters extracted from the continuous records (amplitude and interevent time interval), and these data were converted to probability density functions for comparison. Synaptic events per period were detected using a threshold crossing of the derivative with parameters set for each cell and kept constant for the whole session (Mini Analysis Program; Synaptosoft Inc., Leonia, NJ). The events detected were then visually inspected to remove electrical artifacts before final analysis. Their peak amplitude and 10–90% rise time were measured, and the decay phase of individual events could be fitted by one exponential. Individual EPSCs that did not overlap with other events were selected at random and averaged together to form composite EPSCs for analysis. All results are given as mean ± SD. The large sample approximation of the Kolmogorov–Smirnoff test was used to compare the distributions of sIPSC, mIPSC, sEPSC, and mEPSC parameters between individual representative neurons. Paired or unpaired Student's two-tailed *t* test was used to compare group results. Statistical significance was defined as $p < 0.05$.

Drugs. CNQX and AP-5 were obtained from Tocris Cookson (Ballwin, MO); TTX, BMI, and picrotoxin were from Sigma (St. Louis, MO).

RESULTS

Histological effects

Histological abnormalities found in the irradiated rats have been described in detail previously (Riggs et al., 1956; Cowan and Geller, 1960; Roper et al., 1995). All slices used in this study demonstrated cortical dysplasia and subcortical neuronal heterotopia. Dyplastic cortex (DC) was characterized by thinning of the cortex with loss of lamination and loss of the normal orientation of some pyramidal cells with respect to the pial surface (Fig. 1*B*). DC and heterotopic gray matter were easily visualized with a low-power objective (10×) at the time of physiological recordings using IR-DIC videomicroscopy. Cresyl violet staining of some fixed slices was performed after recording to confirm these changes.

Basic membrane properties in pyramidal neurons

Whole-cell recordings were performed in the somatosensory cortex overlying the lateral ventricle. In control cortex we recorded from neurons in superficial layers (II/III) and in layer V. In DC we recorded from neurons throughout the cortical mantle. Pyramidal neurons were identified using morphological properties of their triangular somata and prominent apical dendrites under IR-DIC videomicroscopy using a 40× objective. As shown in Figure 1*A*, recorded cells filled with biocytin had apical and basal dendrites with many spines and main axons extending to the underlying white matter. Morphological features of pyramidal cells in DC were similar to those of control pyramidal cells, although the orientation of the neuron with respect to the pial surface was sometimes abnormal. No systematic analysis of dendritic or axonal distribution or branching patterns was performed; therefore, the possibility of more subtle structural differences between pyramidal cells in control and dysplastic cortex cannot be excluded. With step-wise depolarization in whole-cell current-clamp recordings, all pyramidal neurons tested (control, $n = 24$; DC, $n = 22$) responded initially with a high frequency of action potentials (APs), adapting to a lower, sustained frequency (Fig. 1*C*) as described for regular spiking cells (McCormick et al., 1985; Chagnac-Amitai and Connors, 1989). The resting potentials in all neurons recorded were more negative than −60 mV. Membrane and AP properties of neurons from layers II/III and V in control neocortex were not different, and these values were not different from those observed in the pyramidal neurons of DC (Table 1).

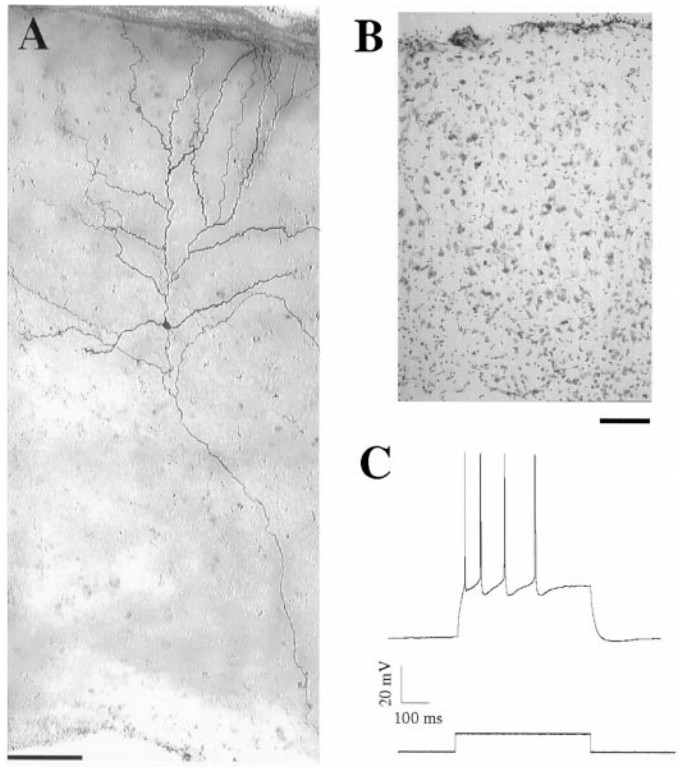

Figure 1. Morphological and physiological properties of a pyramidal neuron in dysplastic cortex. *A*, Composite videomicrograph of a representative biocytin-filled pyramidal cell with the soma lying in the center of the dysplastic cortex, dendrites extending to the pial surface (*top*), and the axon extending into the white matter. Scale bar, 100 μm. *B*, Photomicrograph of a cresyl violet-stained section of dysplastic cortex (40 μm thick) demonstrating thinning of the cortex, loss of laminar organization, and loss of orientation of pyramidal cells (pial surface is at *top*) Scale bar, 100 μm. *C*, Current-clamp recording (*top trace*) of a pyramidal neuron from dysplastic cortex demonstrating the response to depolarizing current (*bottom trace*). Elicited action potentials show frequency adaptation that is indicative of a regular spiking neuron.

Impaired GABAergic synaptic transmission in dysplastic cortex

Whole-cell voltage-clamp recordings were made from pyramidal neurons in dysplastic and control neocortex. Spontaneously occurring inward currents were observed at a holding potential of −60 mV in the presence of CNQX (10 μM) and AP-5 (50 μM). These currents were completely blocked by the $GABA_A$ receptor antagonists picrotoxin (100 μM) and BMI (10 μM), indicating that the synaptic currents were GABAergic. The measured amplitude and frequency of these currents showed no consistent developmental change in the cells from animals aged from postnatal day 28 (P28) to P35 (data not shown), and the kinetics, amplitude, and frequency of sIPSCs between layer II/III and V pyramidal neurons in control neocortex were not significantly different (Table 1). In this study, we grouped neurons from layers II/III and V together in the statistical analysis of IPSCs and EPSCs.

As shown in Figure 2*A*, the frequency of sIPSCs in pyramidal neurons from DC was reduced in comparison with control neurons. However, the 10–90% rise time (control, 1.75 ± 0.12 msec; $n = 20$; DC, 1.88 ± 0.11 msec; $n = 19$; $p = 0.42$) and the decay time constant (control, 10.96 ± 0.61 msec; $n = 20$; DC, 11.47 ± 0.82 msec; $n = 19$; $p = 0.64$) of sIPSCs were not different between

Table 1. Membrane properties and postsynaptic currents in the pyramidal neurons of cortex

	Control pyramidal neuron		DC pyramidal neuron
	Layer II/III	Layer V	
Membrane properties			
V_m (mV)	−67.2 ± 2.8	−69.6 ± 3.1	−68.5 ± 2.6
R_a (mΩ)	16.3 ± 1.2	15.9 ± 1.5	14.7 ± 1.8
R_m (mΩ)	203 ± 15	222 ± 18	211 ± 20
n	14	10	22
sIPSCs			
Amp (pA)	33.88 ± 1.39	34.51 ± 1.2	22.4 ± 1.77*
Fre (Hz)	13.19 ± 0.88	13.73 ± 0.94	4.07 ± 0.46*
RT (msec)	1.85 ± 0.17	1.63 ± 0.18	1.88 ± 0.11
τ (msec)	10.64 ± 0.81	11.36 ± 0.98	11.4 ± 0.82
n	11	9	19
sEPSCs			
Amp (pA)	22.94 ± 1.02	21.78 ± 1.02	28.8 ± 0.92*
Fre (Hz)	2.84 ± 0.29	3.11 ± 0.28	5.49 ± 0.47*
RT (msec)	1.91 ± 0.11	1.77 ± 0.16	2.02 ± 0.16
τ (msec)	8.00 ± 0.43	7.82 ± 0.68	7.38 ± 0.7
n	14	11	28

DC, Dysplastic cortex; V_m, resting membrane potential; R_a, access resistance; R_m, membrane resistance; Amp, amplitude; Fre, frequency; RT, 10–90% rise time; τ, decay time constant.

*$p < 0.001$.

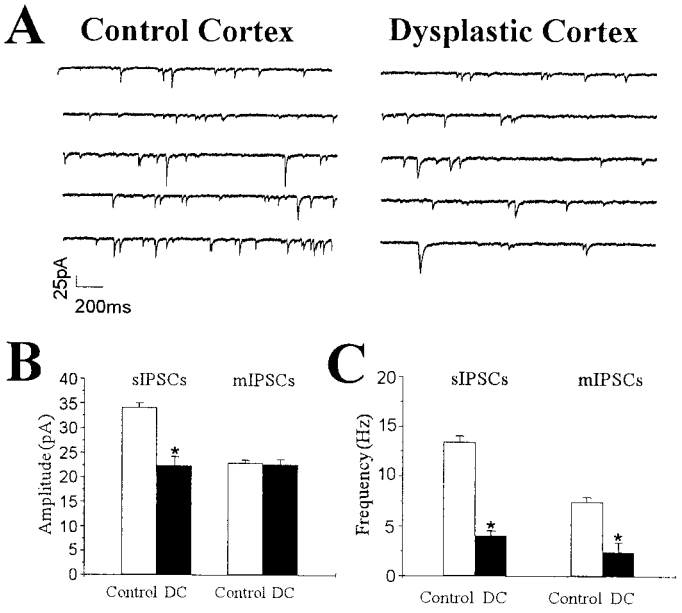

Figure 2. Decreased amplitude and frequency of sIPSCs from pyramidal neurons in dysplastic cortex. *A*, Representative traces of voltage-clamp recordings from pyramidal neurons in control neocortex and dysplastic cortex in the presence of AP-5 (50 μM) and CNQX (10 μM). *B, C*, Group comparison of amplitude and frequency of sIPSCs and mIPSCs from pyramidal neurons in control neocortex and DC. Graphs show data for amplitude (*B*) and frequency (*C*) of sIPSCs (*left*) and mIPSCs (*right*). *B*, Mean values of sIPSC amplitude were decreased in DC ($p < 0.001$), but the mIPSC amplitude was not different ($p = 0.83$). *C*, Mean frequencies of both sIPSCs and mIPSCs were significantly reduced in DC ($p < 0.001$ for both measures).

control and dysplastic cortex. Mean amplitude and frequency of sIPSCs in pyramidal neurons from control ($n = 20$) and dysplastic cortex ($n = 19$) are shown in Figure 2, *B* and *C*. Both amplitude and frequency were significantly reduced by 35 and 70%, respectively, in pyramidal neurons from DC.

Miniature IPSCs resulting from the spontaneous, action potential-independent release of GABA from individual vesicles in the axon terminals were recorded in the presence of TTX (1 μM) (Fig. 3*A*). To determine whether inhibitory synaptic activity was impaired in DC, the amplitude, frequency, and kinetics of mIPSCs from pyramidal cells in DC were compared with those from pyramidal cells in control neocortex. The decay time constant of mIPSCs was not changed between the two groups (control, 10.1 ± 0.72 msec; $n = 17$; DC, 9.35 ± 0.78 msec; $n = 18$; $p = 0.48$). Also, there was no significant difference in the 10–90% rise time of mIPSCs (control, 1.75 ± 0.12 msec, $n = 17$; DC, 1.71 ± 0.13 msec; $n = 18$; $p = 0.67$). Amplitude distribution histograms were similar between representative pyramidal neurons from control and dysplastic cortex (Fig. 3*B*). The mean amplitude of mIPSCs (Fig. 2*B*) was also not different between control ($n = 17$) and dysplastic cortex ($n = 18$). However, cumulative probability curves demonstrated an increase of the interevent interval in DC when representative neurons were compared (Fig. 3*D*). In the group comparison, the mean frequency of mIPSCs was significantly reduced by 66% in DC ($n = 17$) compared with control ($n = 18$) neocortex (Fig. 2*C*).

Decreased monosynaptic evoked IPSCs in pyramidal neurons from dysplastic cortex

At a holding potential of −60 mV, single-pulse stimulation was applied by a bipolar platinum-iridium electrode positioned 150–200 μm away from the recorded soma to directly activate local interneurons. Monosynaptic evoked IPSCs (eIPSCs) of pyramidal neurons were recorded in the presence of CNQX (10 μM) and AP-5 (50 μM), and stimulus amplitudes were increased in intensity (0–500 μA) until they reached a maximal response. To verify that monosynaptic eIPSCs were $GABA_A$-mediated, in some experiments a $GABA_A$ receptor antagonist (BMI, 10 μM, or picrotoxin, 100 μM) was applied to the bath solution, showing a complete and reversible abolishment of evoked postsynaptic currents (data not shown). Evoked IPSCs displayed a fast-onset inward current with a small delay after the stimulation (Fig. 4*A*). Failures were more frequent at lower intensities. In pyramidal neurons from DC, mean rise time and decay time constants were 5.2 ± 1.12 and 25.68 ± 2.34 msec ($n = 20$), respectively, which were not significantly different from those in control neurons. However, the mean maximal amplitude of monosynaptic eIPSCs was significantly decreased by 48% in pyramidal neurons from DC ($n = 16$) compared with controls ($n = 20$; failures not included) (Fig. 4*B*).

Absence of paired pulse depression in pyramidal neurons from dysplastic cortex

To examine excitatory synaptic transmission in DC, neocortical pyramidal neurons were voltage-clamped at −65 mV, close to the Cl^- equilibrium potential, with potassium gluconate intracellular solution. Evoked EPSCs (eEPSCs) were induced by placing a bipolar platinum-iridium electrode in the white matter beneath the neocortex, showing increased inward currents with an increase in the stimulation intensity (0–500 μA). The average 10–90% rise time and decay time constants were 1.85 ± 0.09 and 7.9 ± 0.38 msec ($n = 16$), respectively, in control neocortex. Bath perfusion of CNQX (10 μM) and AP-5 (50 μM) completely and reversibly blocked the eEPSCs. We observed that the fast-onset inward peak current of eEPSCs was usually followed by a group of high-frequency, inward currents in pyramidal cells from DC (Fig. 5*A*), but this activity was rare in controls (control, 3 of 16 cells; DC, 15 of 18 cells). The delayed inward discharges could be abolished by bath application of CNQX and AP-5, indicating that they are glutamate-mediated events. Evoked EPSCs in pyramidal neurons from DC ($n = 14$) showed a 52% increase in amplitude compared with controls ($n = 22$; Fig. 5*B*), and the total charge transfer during eEPSCs was significantly increased in pyramidal neurons from DC compared with controls (Fig. 5*C*). The 10–90% rise time was not significantly changed in DC.

To examine the competency of feedback inhibition in the neural circuits of DC, paired pulse stimulation (interpulse interval, 20 msec) was applied while eEPSCs were recorded in pyramidal cells

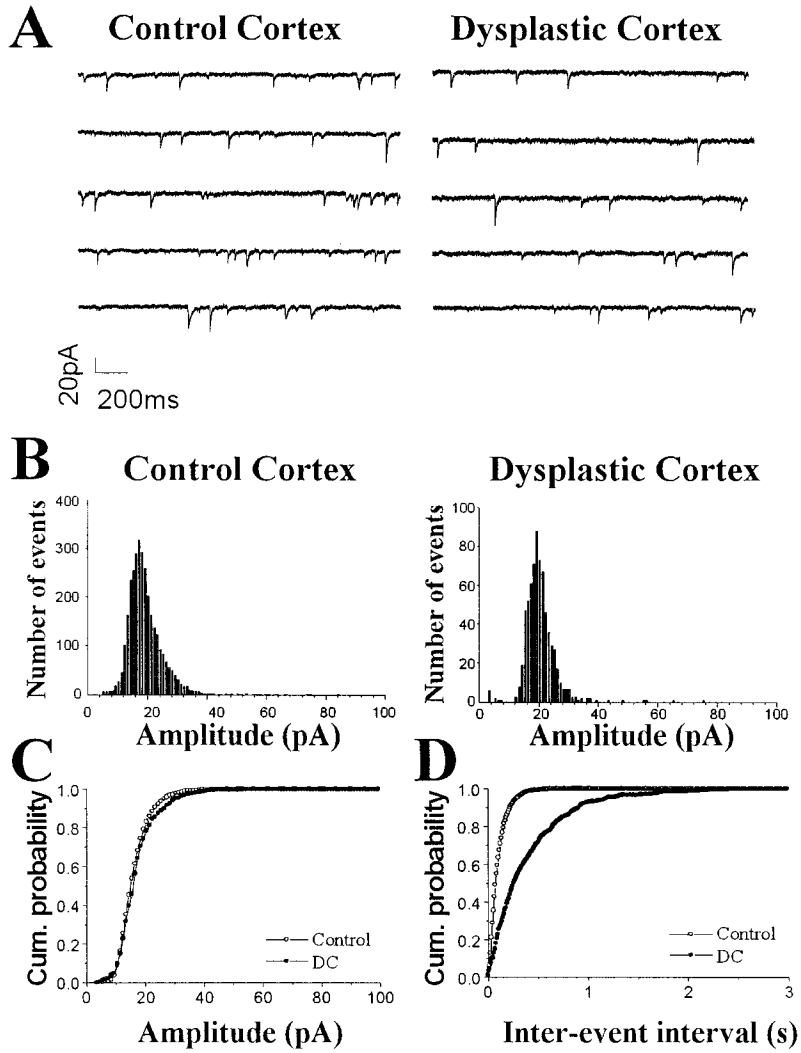

Figure 3. Decreased frequency of mIPSCs in pyramidal neurons from dysplastic cortex. *A*, Representative voltage-clamp recordings of mIPSCs from pyramidal neurons from control and dysplastic cortex in the presence of AP-5 (50 μM), CNQX (10 μM), and TTX (1 μM). *B*, Distribution histograms of mIPSC amplitude from these cells show similar patterns. Normalized cumulative probability curves show no difference between control and dysplastic cortex for mIPSC amplitude (*C*; $p = 0.16$), but the interevent interval (*D*) is shifted to the right (consistent with decreased frequency) in the neuron from dysplastic cortex ($p < 0.0001$).

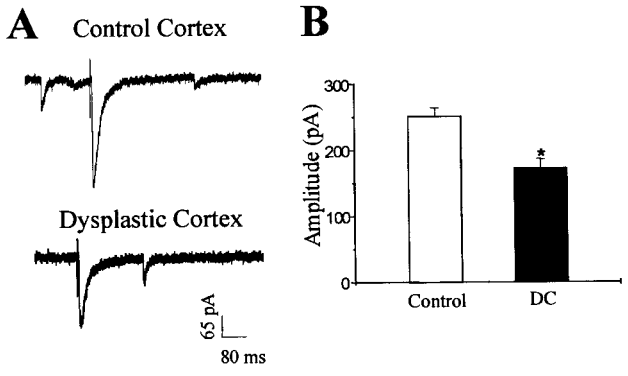

Figure 4. Monosynaptic evoked IPSCs recorded from pyramidal neurons from control and dysplastic cortex in the presence of AP-5 (50 μM) and CNQX (10 μM). *A*, Representative recordings of monosynaptic eIPSCs show a smaller response in the neuron from dysplastic cortex (*bottom trace*) compared with the control neuron (*top trace*). *B*, Group comparison of data from control and dysplastic cortex shows a significant reduction in monosynaptic eIPSC amplitude in pyramidal neurons from dysplastic cortex ($p < 0.002$).

at a holding potential of −65 mV. As shown in Figure 6*A*, the second eEPSC amplitude was smaller than the first response in control neocortex. However, the second synaptic response was increased compared with the first one in DC, suggesting an impairment of feedback inhibition in DC neuronal circuits. This difference was maintained when group data from control neocortex ($n = 14$) and DC ($n = 16$) were compared (Fig. 6*B*).

Enhanced excitatory synaptic transmission in pyramidal neurons from dysplastic cortex

Spontaneous EPSCs were recorded from neocortical pyramidal neurons voltage-clamped at −65 mV (Fig. 7*A*). Bath application of CNQX and AP-5 completely and reversibly abolished the spontaneously occurring inward currents observed at this holding potential. As observed in IPSCs, the amplitude and frequency of EPSCs did not change with age (P28–P35) and were not different between layer II/III and V pyramidal neurons (Table 1). The 10–90% rise times (control, 1.85 ± 0.09 msec; $n = 25$; DC, 2.02 ± 0.16 msec; $n = 28$; $p > 0.05$) and decay times (control, 7.92 ± 0.38 msec; $n = 25$; DC, 7.38 ± 0.7 msec; $n = 28$; $p > 0.05$) of sEPSCs were not different between pyramidal cells from control neocortex and DC. In representative neurons, the distribution of sEPSCs showed larger amplitudes in DC than in control neurons (Figs. 7*B*), and cumulative probability curves were shifted to larger amplitudes (Fig. 7*C*). In the group analysis, the mean sEPSC amplitude was increased by 42% in pyramidal neurons from DC ($n = 28$) compared with controls ($n = 25$) (Fig. 8*A*). In representative neurons, cumulative probability curves showed a decrease in interevent intervals for sEPSCs in pyramidal cells from DC (Fig. 7*D*). Group comparisons showed that mean sEPSC frequency was significantly higher in DC ($n = 28$) compared with controls ($n = 25$) (Fig. 8*B*).

Miniature EPSCs were recorded in the presence of TTX (1 μM) from pyramidal cells voltage-clamped at −65 mV to examine presynaptic or postsynaptic mechanisms of increased excitability in the neuronal circuits of dysplastic cortex. In contrast to sEPSCs, there was no difference in mean amplitude or frequency of mEPSCs

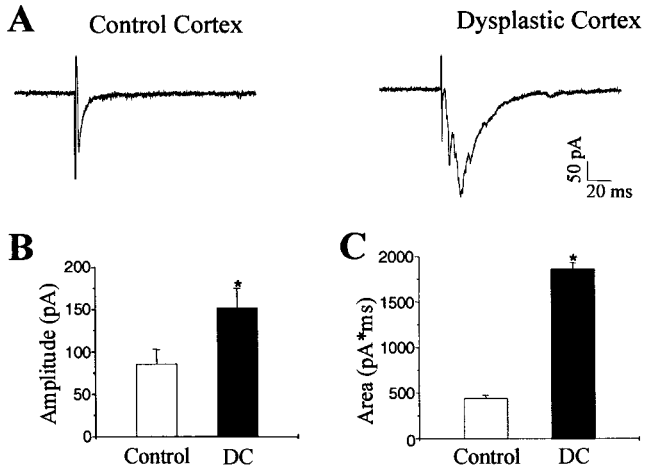

Figure 5. Evoked EPSCs recorded at the reversal potential of GABAgeric currents in pyramidal neurons from control and dysplastic cortex. *A*, Representative recordings of eEPSCs in pyramidal neurons from control and dysplastic cortex. Evoked EPSCs from dysplastic cortex typically demonstrated a complex response comprising multiple inward currents. *B*, Group comparison of data from control and dysplastic cortex shows an increase in eEPSC peak amplitude in dysplastic cortex ($p < 0.001$). *C*, The averaged area of eEPSCs in dysplastic cortex was also significantly increased ($p < 0.001$).

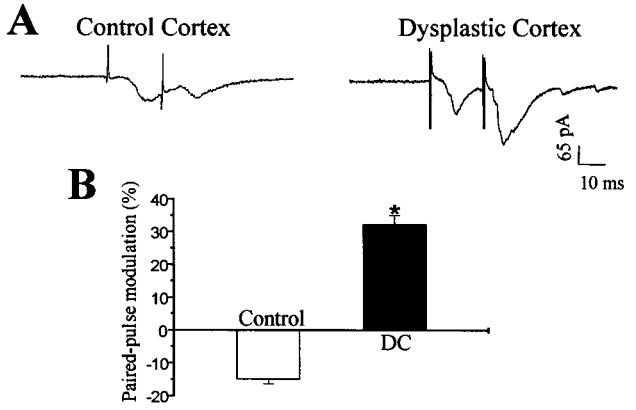

Figure 6. Paired pulse modulation of evoked EPSCs recorded from pyramidal neurons in control and dysplastic cortex with an interpulse interval of 20 msec. *A*, Representative recordings of paired eEPSCs in pyramidal cells from control and dysplastic cortex show that the amplitude of the second response was reduced in the control neuron but increased in the neuron from dysplastic cortex. *B*, Group data from control and dysplastic cortex demonstrate an absence of paired pulse depression in dysplastic cortex ($p < 0.001$).

between pyramidal neurons from control ($n = 15$) and dysplastic ($n = 12$) cortex (Fig. 8). There was also no difference in rise time, decay time, or distribution of mEPSC amplitude or interevent interval. Therefore, blocking action potential-dependent activity abolished the increased spontaneous excitatory activity in pyramidal neurons from DC.

DISCUSSION

This study has demonstrated significant impairment of inhibition in the *in utero* irradiation model of cortical dysplasia. The reduction in frequency of miniature IPSCs recorded from pyramidal cells with no difference in amplitude suggests that the principal abnormality is presynaptic rather than postsynaptic. This could result from an impaired release mechanism from the presynaptic terminals or simply from a reduction in the number of GABAergic terminals on the pyramidal cells. This second explanation is supported by previous studies from this laboratory that showed a reduction in density of parvalbumin- and calbindin D28k-immunoreactive neurons in dysplastic cortex from irradiated rats (Roper et al., 1999), because a reduced number of inhibitory neurons would likely result in a reduced number of inhibitory connections by these neurons onto adjacent pyramidal cells. In addition, the similar frequency of both spontaneous and miniature IPSCs may indicate a relatively low level of spontaneous activity in inhibitory interneurons in dysplastic cortex.

Decreases in paired pulse inhibition and monosynaptic evoked IPSCs also provide evidence for impaired inhibition in dysplastic cortex but do not give any additional information regarding the specific mechanisms of this impairment. In this study, paired pulse depression of excitatory postsynaptic responses was selected as a common measure of cortical inhibition (Burdette and Gilbert, 1995; Ramoa and Sur, 1996) to either support or contradict the spontaneous IPSC results. Whole-cell recordings from paired cortical neurons have confirmed that, with an interstimulus interval of 20 msec, pyramidal cell pairs generally show paired pulse depression, whereas pyramidal interneuron pairs show paired pulse facilitation (Thomson, 1997). However, short-term synaptic plasticity is affected by many variables, such as presynaptic release probability (Oleskevich et al., 2000), postsynaptic receptors and cell properties (Rozov and Burnashev, 1999), and presynaptic $GABA_B$ receptors (Deisz, 1999), and other explanations for our reported changes in paired pulse depression are possible.

In this study we used neurons from both supragranular and infragranular layers of control neocortex for comparison with neurons from DC. DC in this model has no clear laminar pattern, so there are no anatomic cues on which to base a comparison between the same cortical layers in both the control and experimental groups. Neurons in DC are most likely to represent neurons that should have assumed an infragranular location, because the irradiation occurs at a time when the early cortical plate has already formed, and neurons destined for the deeper layers arrive first in cortical development. The irradiation treatment kills immature, migrating neurons (Bayer and Altman, 1991) as well as radial glia (Roper et al., 1997a) with relative sparing of the cortical plate neurons and the neuroepithelium. After irradiation, some neurons are trapped in the periventricular and subcortical regions and go on to form neuronal heterotopias, but some may still migrate out to the cortical plate. Therefore the resultant dysplastic cortex (as opposed to the underlying heterotopic gray matter) probably represents an amalgam of neocortical neurons with a heavier representation from neurons originally destined for the deeper cortical layers. Because of these factors, it is difficult to assign a specific category of neurons from control neocortex to serve as the appropriate control group. For this reason we have studied pyramidal cells (which can clearly be identified morphologically in both control and dysplastic neocortex) from both supragranular and infragranular layers in control neocortex as the comparison group. This raises the possibility that our study could produce a spurious result if, for instance, one group of control neurons had a significantly higher frequency of miniature IPSC's when the appropriate comparison was actually with the control subset with a lower frequency. To address this problem we compared the supragranular control neurons with the infragranular control neurons and found no differences between the two groups with respect to basic membrane properties or amplitude or frequency of sIPSCs or sEPSCs. On the basis of these findings it seems appropriate to use the pooled data from supragranular and infragranular neurons in control neocortex for comparison with neurons from DC in this study.

The findings of partial loss of inhibition in this model are consistent with observations in human cortical dysplasia. Two groups have reported a qualitative reduction in inhibitory interneurons in specimens of human focal cortical dysplasia surgically resected for the treatment of intractable epilepsy (Ferrer et al., 1992, 1994; Spreafico et al., 1998). In addition, physiological abnormalities have been reported in human cortical dysplasia. Surface recordings (electrocorticography) from focal cortical dysplasia can show continuous ictal activity that is rarely seen in other types epilepsy (Palmini et al., 1995). In addition, *in vitro* brain slices of human dysplastic cortex demonstrate prolonged epileptiform dis-

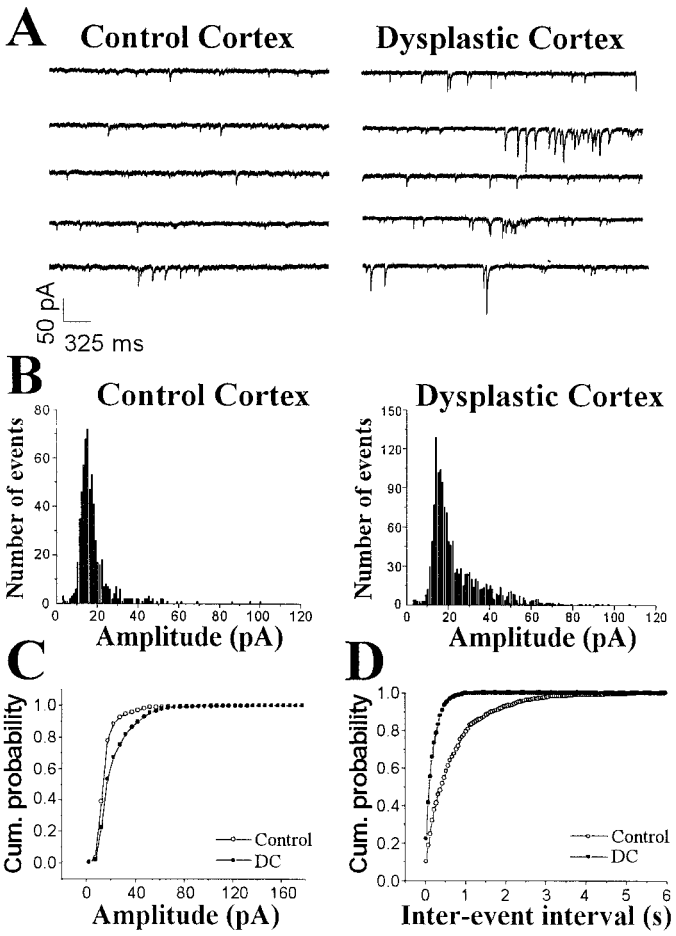

Figure 7. Increased amplitude and frequency in sEPSCs in pyramidal neurons from control and dysplastic cortex. *A*, Representative voltage-clamp recordings demonstrate a significant increase in amplitude and frequency of sEPSCs in the pyramidal neuron from dysplastic cortex compared with the control neuron. *B*, Amplitude distribution histograms of sEPSCs from pyramidal neurons from control and dysplastic cortex show that sEPSCs were skewed toward larger amplitudes, especially in dysplastic cortex. *C*, Normalized cumulative probability curves of sEPSC amplitude show that values from the dysplastic cortex neuron were significantly shifted to the right ($p < 0.0001$), indicating an increase in sEPSC amplitude in this cell. *D*, Normalized cumulative probability curves of interevent intervals are significantly shifted to the left in the pyramidal neuron from dysplastic cortex compared with the control neuron ($p < 0.0001$), indicating an increase in sEPSC frequency in the dysplastic cortex neuron.

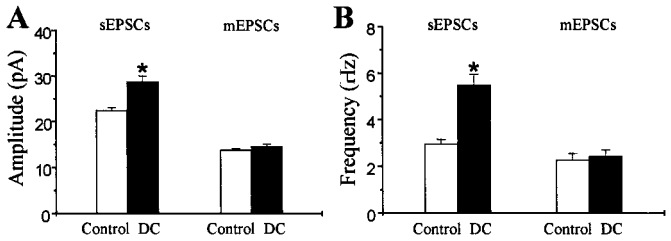

Figure 8. Group comparisons of amplitude and frequency of sEPSCs and mEPSCs from pyramidal neurons from control and dysplastic cortex. Graphs show data for amplitude (*A*) and frequency (*B*) of sEPSCs (*left*) and mEPSCs (*right*). Mean values of sEPSC amplitude were increased in dysplastic cortex ($p < 0.001$), but there was no difference in mean mEPSC amplitude between the two groups ($p = 0.21$). Mean sEPSC frequency was increased in dysplastic cortex ($p < 0.001$), but there was no difference in mean frequency of mEPSCs between the two groups ($p = 0.67$).

charges that are not seen from "control" human temporal neocortex that is removed during anterior temporal lobectomy for medial temporal lobe epilepsy (Mattia et al., 1995). Although these physiological abnormalities document an increased propensity for epileptiform activity, they do not specifically indicate impaired inhibition, and other mechanisms could explain these findings.

There are several other animal models of cortical dysplasia that have been studied. *In utero* administration of the alkylating agent methylazoxymethanol acetate produces histological changes similar to those in the *in utero* irradiation model. Physiological abnormalities in this model have included an increase in the number of intrinsically bursting neurons in the hippocampus (Baraban and Schwartzkroin, 1995) and neocortex (Sancini et al., 1998). In the current study, we did not find intrinsically bursting neurons in either control or dysplastic neocortex. Intrinsically bursting pyramidal neurons were originally described in layer V of normal neocortex using sharp intracellular microelectrodes (McCormick et al., 1985; Chagnac-Amitai and Connors 1989). Because of the large tip diameter of microelectrodes used in whole-cell patch-clamp recordings, the electrode-filling solution communicates freely with the cytoplasm of the recorded cell. Because intrinsic firing properties are significantly affected by intracellular calcium levels (Friedman and Gutnick, 1989), it is possible that alterations in intracellular calcium attributable to washout or buffering from the microelectrode-filling solution make detection of intrinsically bursting cells unlikely. In addition to this, there are differences in age of the animals and the temperature of the recording chambers between these studies that might affect intrinsic firing patterns. Of note, Kawaguchi (1993) used whole-cell patch-clamp recording techniques similar to those used in the current study in control neocortex and also found no intrinsically bursting neurons in rat frontal cortex. Additional studies using sharp intracellular microelectrodes may provide better detection and quantification of intrinsically bursting cells in DC.

One model of focal cortical dysplasia involves creating a cortical freeze lesion on P0 or P1 that persists as a microsulcus. These animals develop an area of hyperexcitable cortex just adjacent to the actual lesion, the paramicrogyral cortex. Although there is a loss of parvalbumin-immunoreactive neurons in supragranular layers of the microsulcus and adjacent cortex in early postnatal development, this deficit recovers by P21. There is a permanent decrease in parvalbumin-immunoreactive neurons in the infragranular cortex in the microgyrus and paramicrogyral cortex in this model (Rosen et al., 1998). Spontaneous and evoked IPSCs are increased in amplitude but not frequency in the paramicrogyral cortex (Prince et al., 1997), and current theories on epileptogenesis in this model involve synaptic reorganization with exuberant thalamocortical connections in the paramicrogyral cortex attributable to loss of normal targets in the microsulcus (Jacobs et al., 1999). DeFazio and Hablitz (1999, 2000) have provided evidence for a delay or arrest of normal maturation of GABA receptors (DeFazio and Hablitz, 1999) and NMDA receptors (DeFazio and Hablitz, 2000) in neurons of the paramicrogyral cortex in this model.

In addition to reduced inhibitory currents, we have also demonstrated an increase in the frequency of sEPSCs in pyramidal cells from DC. This difference was abolished when action potentials were blocked with TTX. This suggests that the increased sEPSCs did not represent a primary increase in the number of excitatory presynaptic terminals on the pyramidal cells or a primary alteration in glutamatergic receptors. It could be a consequence of reduced inhibition in the local circuit, because a reduction of inhibitory tone would allow excitatory cells to fire more often. It could also result from an increase in the number of intrinsically bursting neurons in dysplastic cortex.

This study is the first to quantitatively demonstrate a physiological impairment in inhibition in an animal model of hyperexcitable dysplastic cortex. Paired with previous data that showed a persistent, selective reduction of inhibitory interneurons in the same areas (Roper et al., 1999), these results demonstrate a selective vulnerability of the inhibitory system to *in utero* irradiation. We do not know whether this is a direct effect of the radiation on immature neurons that would have become inhibitory neurons or whether it is a secondary effect of the treatment. It is even possible

that the inhibitory neurons are still present but misplaced. Preliminary studies have shown inhibitory interneurons in subcortical and periventricular heterotopic gray matter in these animals, but no quantitative studies have been performed (Roper and Houser, 1992). Whole-cell recordings from heterotopic pyramidal neurons in this model have shown the presence of inhibitory activity, but this has not been quantified (Smith et al., 1999).

The majority of inhibitory interneurons of the neocortex originate outside the cortical mantle in the lateral and median ganglionic eminence (Anderson et al., 1997, 1999; Tamamiki et al., 1997). This necessitates a longer migratory pathway to the cortical plate and may make these immature inhibitory neurons more susceptible to *in utero* injury, because migrating neurons are among the most vulnerable to *in utero* irradiation (Altman et al., 1968; Bayer and Altman, 1991). Alternatively, the putative inhibitory neurons either may arrive at the cortical plate and not develop their appropriate phenotype or may die off during development because of some secondary abnormality in the dysplastic cortex such as increased excitatory activity or alterations in subcortical afferents. The current data do not provide evidence to address these questions, and further studies are needed. At this point, these studies have demonstrated a selective vulnerability of inhibitory interneurons to *in utero* injury that may have far-reaching implications for other disorders of cortical development.

REFERENCES

Altman J, Anderson WJ, Wright KA (1968) Differential radiosensitivity of stationary and migratory primitive cells in the brains of infant rats. Exp Neurol 22:52–74.

Anderson SA, Eisenstat DD, Shi L, Rubenstein JLR (1997) Interneuron migration from basal forebrain to neocortex: dependence on *Dlx* genes. Science 278:472–476.

Anderson S, Mione M, Yun K, Rubenstein JLR (1999) Differential origins of neocortical projection and local circuit neurons: role of Dlx genes in neocortical interneuronogenesis. Cereb Cortex 9:646–654.

Baraban SC, Schwartzkroin PA (1995) Electrophysiology of CA1 pyramidal neurons in an animal model of neuronal migration disorders: prenatal methylazoxymethanol treatment. Epilepsy Res 22:145–156.

Bayer SA, Altman J (1991) Neocortical development. New York: Raven.

Burdette LJ, Gilbert ME (1995) Stimulus parameters affecting paired-pulse depression of dentate granule cell field potentials. I. Stimulus intensity. Brain Res 680:53–62.

Chagnac-Amitai Y, Connors BW (1989) Synchronized excitation and inhibition driven by intrinsically bursting neurons in neocortex. J Neurophysiol 62:1149–1162.

Cowan D, Geller LM (1960) Long-term pathological effects of prenatal X-irradiation on the central nervous system of the rat. J Neuropathol Exp Neurol 19:488–527.

DeFazio RA, Hablitz JJ (1999) Reduction of zolpidem sensitivity in a freeze lesion model of neocrtical dysgenesis. J Neurophysiol 81:404–407.

DeFazio RA, Hablitz JJ (2000) Alterations in NMDA receptors in a rat model of cortical dysplasia. J Neurophysiol 83:315–321.

Deisz RA (1999) $GABA_B$ receptor-mediated effects in human and rat neocortical neurones in vitro. Neuropharmacology 38:1755–1766.

Ferrer I, Pineda M, Tallada M, Oliver B, Russi A, Oller L, Noboa R, Zujar MJ, Alcantara S (1992) Abnormal local-circuit neurons in epilepsia partialis continua associated with focal cortical dysplasia. Acta Neuropathol (Berl) 83:647–652.

Ferrer I, Oliver B, Russi A, Casas R, Rivera R (1994) Parvalbumin and calbindin-D28k immunocytochemistry in human neocortical epileptic foci. J Neurol Sci 123:18–25.

Friedman A, Gutnick MJ (1989) Intracellular calcium and control of burst generation in neurons of guinea-pig neocortex in vitro. Eur J Neurosci 4:374–381.

Hirabayashi S, Binnie CD, Janota I, Polkey CE (1993) Surgical treatment of epilepsy due to cortical dysplasia: clinical and EEG findings. J Neurol Neurosurg Psychiatry 56:765–770.

Jacobs KM, Hwang BJ, Prince DA (1999) Focal epileptogenesis in a rat model of polymicrogyria. J Neurophysiol 81:159–173.

Kawaguchi Y (1993) Groupings of nonpyramidal and pyramidal cells with specific physiological and morphological characteristics in rat frontal cortex. J Neurophysiol 69:416–431.

Mattia D, Olivier A, Avoli M (1995) Seizure-like discharges recorded in human dysplastic neocortex maintained in vitro. Neurology 45:1391–1395.

McCormick DA, Connors BW, Lighthall JW, Prince DA (1985) Comparative electrophysiology of pyramidal and sparsely spiny stellate neurons of the neocortex. J Neurophysiol 54:782–806.

Mischel PS, Nguyen LP, Vinters HV (1995) Cerebral cortical dysplasia associated with pediatric epilepsy. Review of neuropathologic features and proposal for a grading system. J Neuropathol Exp Neurol 54:137–153.

Oleskevich S, Clements J, Walmsley B (2000) Release probability modulates short-term plasticity at a rat giant terminal. J Physiol (Lond) 524:513–523.

Palmini A, Andermann F, Olivier A, Tampieri D, Robitaille Y, Andermann E, Wright G (1991) Focal neuronal migration disorders and intractable partial epilepsy: a study of 30 patients. Ann Neurol 30:741–749.

Palmini A, Gambardella A, Andermann F, Dubeau F, da Costa JC, Olivier A, Tampieri D, Gloor P, Quesney F, Andermann E, Paglioli E, Paglioli-Neto E, Coutinho C, Leblanc R, Kim HI (1995) Intrinsic epileptogenicity of human dysplastic cortex as suggested by corticography and surgical results. Ann Neurol 37:476–487.

Prince DA, Jacobs KM, Salin PA, Hoffman S, Parada I (1997) Chronic focal neocortical epileptogenesis: does inhibition play a role? Can J Physiol Pharmacol 75:500–507.

Ramoa AS, Sur M (1996) Short-term synaptic plasticity in the visual cortex during development. Cereb Cortex 6:640–646.

Raymond AA, Fish DR, Sisodiya SM, Alsanjari N, Stevens JM, Shorvon SD (1995) Abnormalities of gyration, heterotopias, tuberous sclerosis, focal cortical dysplasia, microdysgenesis, dysembryoplastic neuroepithelial tumor and dysgenesis of the archicortex in epilepsy. Clinical, EEG and neuroimaging features in 100 adult patients. Brain 118:629–660.

Riggs HE, McGrath JJ, Schwartz HP (1956) Malformation of the adult brain (albino rat) resulting from prenatal irradiation. J Neuropathol Exp Neurol 15:432–447.

Roper SN, Houser CR (1992) Experimentally-induced heterotopias contain GAD-immunoreactive neurons. Epilepsia 33[Suppl 3]:75A.

Roper SN, Gilmore RL, Houser CR (1995) Experimentally induced disorders of neuronal migration produce an increased propensity for electrographic seizures in rats. Epilepsy Res 21:205–219.

Roper SN, Abraham LA, Streit WJ (1997a) Exposure to in utero irradiation produces disruption of radial glia in rats. Dev Neurosci 19:521–528.

Roper SN, King MA, Abraham LA, Boillot MA (1997b) Disinhibited in vitro neocortical slices containing experimentally induced cortical dysplasia demonstrate hyperexcitability. Epilepsy Res 26:443–449.

Roper SN, Eisenschenk S, King MA (1999) Reduced density of parvalbumin- and calbindin D28k-immunoreactive neurons in experimental cortical dysplasia. Epilepsy Res 37:63–71.

Rosen GD, Jacobs KM, Prince DA (1998) Effects of neonatal freeze lesions on expression of parvalbumin in rat neocortex. Cereb Cortex 8:753–761.

Rozov A, Burnashev N (1999) Polyamine-dependent facilitation of postsynaptic AMPA receptors counteracts paired-pulse depression. Nature 401:594–598.

Sancini G, Franceschetti S, Battaglia G, Colacitti C, Di Luca M, Spreafico R, Avanzini G (1998) Dysplastic neocortex and subcortical heterotopias in methylazoxymethanol-treated rats: an intracellular study of identified pyramidal neurones. Neurosci Lett 246:181–185.

Smith BN, Dudek FE, Roper SN (1999) Synaptic responses of neurons in heterotopic gray matter in an animal model of cortical dysgenesis. Dev Neurosci 21:365–373.

Spreafico R, Battaglia G, Arcelli P, Andermann F, Dubeau F, Palmini A, Olivier A, Villemure J-G, Tampieri D, Avanzini G, Avoli M (1998) Cortical dysplasia: an immunocytochemical study of three patients. Neurology 50:27–36.

Tamamiki N, Fujimori KE, Takajui R (1997) Origin and route of tangentially migrating neurons in the developing neocortical intermediate zone. J Neurosci 17:8313–8323.

Taylor DC, Falconer MA, Bruton CJ, Corsellis JAN (1971) Focal dysplasia of the cerebral cortex in epilepsy. J Neurol Neurosurg Psychiatry 34:369–387.

Thomson AM (1997) Activity-dependent properties of synaptic transmission at two classes of connections made by rat neocortical pyramidal axons in vitro. J Physiol (Lond) 502:131–147.